R. G. KIRK
Senior Engineer,
Pratt & Whitney Aircraft,
East Hartford, Conn. Assoc. Mem. ASME

E. J. GUNTER
Associate Professor,
Department of Mechanical Engineering,
University of Virginia,
Charlottesville, Va. Mem. ASME

Transient Response of Rotor-Bearing Systems

The equations of motion necessary to calculate the transient response of a multimass flexible rotor supported by nonlinear, damped bearings are derived from energy principles. Rotor excitation may be the result of imbalance, internal friction, rotor acceleration, nonlinear forces due to any number of bearing or seal stations, and gyroscopic couples developed from skewed disk effects. The method of solution for transient response simulation is discussed in detail and is based on extensive evaluation of numerical methods available for transient analysis. Examples of the application of transient response for the analysis of rotor bearing systems are presented and compared to actual machine performance. Recommendations for the use and extension of the present system simulation model are discussed.

Introduction

THE field of rotor dynamics is becoming of increasing importance in the rotating equipment field. This is due in part to the increased demand for reliable machine performance and reduced maintenance over long periods of operation and under variable operating conditions. The cost of experimental testing makes it practical to consider computer simulation to verify rotor bearing system designs without the necessity of building each design variation considered. Rotor dynamics consists of the study of the following major areas of concern.

1 Undamped critical speed analysis.
2 Steady-state response to imbalance.
3 Methods of calculating the residual imbalance in a given rotor.
4 Stability of rotor-bearing systems as a result of the calculation of damped critical speeds or by the application of stability criteria (such as the Routh criteria).
5 Transient rotor response to imbalance and external forcing functions in addition to detailed studies of self-excited transient behavior.

The transient response analysis of rotor-bearing systems is the most inclusive approach to system analysis since it can be used to obtain information on critical speeds, forced response, stability, impact, and shock loading for systems that have nonlinear force deflection characteristics. The practical usage of a transient response program, however, limits its purpose to the latter three areas of concern. Stability in the usual sense refers to the solution of the dynamic system complex eigenvalues to determine the exponential growth (unstable) or decay (stable) rate. Transient solutions allow this concept of stability to be extended to systems acted upon by varying levels of imbalance. Effects of impact loading arising from blade loss is accurately studied only by a complete time transient solution of an appropriate rotor-system simulation model. Shock loading to the bearing support struc-

Contributed by the Vibration and Sound Committee of the Design Engineering Division of THE AMERICAN SOCIETY OF MECHANICAL ENGINEERS for presentation at the Design Engineering Technical Conference, Cincinnati, Ohio, September 9–12, 1973. Manuscript received at ASME Headquarters, June 6, 1973. Paper No. 73-Det-102.

Copies will be available until June, 1974.

Nomenclature

a = axial distance to first bearing
A = matrix defined by $\alpha_{ij}m_j$
b = axial distance to second bearing
B = matrix defined by $\beta_{ij}I_{Tj}$
(BF) = bearing force
C_i = ith rotor station absolute damping
CI_i = internal friction damping at ith station
C = matrix defined by $\varphi_{ij}m_j$
$(C_x, C_y)_i$ = external torques at ith rotor station
C_{θ_i} = ith station angular damping
D = matrix defined by $\gamma_{ij}I_{Tj}$
e_i = ith mass station eccentricity
$(F_x^{(n)}, F_y^{(n)})$ = column vector of displacements
$(\hat{F}_x, \hat{F}_y)_i$ = generalized external forces at ith station
$(\mathfrak{F}_x, \mathfrak{F}_y)_i$ = external forces minus inertia terms at ith rotor station
$(H_x, H_y)_i$ = external torques minus inertia couples at ith rotor station
$(I_P, I_T)_i$ = polar and transverse moment of inertia at ith station
K_i = external springrate at ith station
$\mathcal{K}_i$ = torsional springrate at ith station

(Continued on next page)

tures may be similarly studied in detail by transient simulation. Recently reports on the development of transient response techniques [1, 2][1] for flexible rotors appeared in the literature. Previous investigations had dealt with single plane analysis of rigid rotors in fluid-film bearings [3–5]. The present analysis presents a discussion of the complete dynamical equations of motion of a flexible rotor shaft using the entire set of flexibility influence coefficients. This is an extension of the analysis of Shen [1] who formulated the problem using only the transverse deflection influence coefficient with approximate gyroscopic moment contributions. The following analysis makes use of the total flexibility matrix to formulate the equations of motion in terms of four degrees of freedom for each rotor mass station. The option to retain gyroscopics only at selected stations where the effect is dominant is easily accounted for in the solution technique.

The present formulation allows many nonlinear effects to be studied in regards to their influence on the dynamic response of flexible rotors. The imbalance response of rotors supported in multilobe or tilting pad bearings is readily obtained. In addition the effects of fluid-film dampers on rotor performance may be investigated. Two brief examples of transient simulation for rotor-bearing analysis are given to demonstrate the usefulness of the approach for analysis of high-speed rotor-bearing response. Recommendations for the use of the simulation model are summarized in the conclusions and are based upon extensive evaluation of the numerical methods available for transient response analysis.

Description of Simulation Model

The large class of rotating machinery operating near or above their first bending critical must be analyzed under the general field of study known as flexible rotor dynamics. A typical rotor in general has multiple bearings and the rotor shaft may have disks or impellers located inboard and outboard to the main bearings. The continuous rotor shaft may be regarded as a series of concentrated mass stations connected by massless elastic shaft. For practical purposes the gyroscopic effects should be included in the analysis of overhung rotor stations but may be neglected in some cases for rotor stations inboard of the main bearings. Although the notation flexible rotor is appropriate, the deflections considered are small in comparison to the dimensions of the rotor and simplified equations for the rotor shaft mechanics may be incorporated into the analysis.

Fig. 1(*a*) represents an idealized rotor system reduced to the model used for the analytical description. This analysis will consider the rotor to be supported on two main bearings which may in turn be elastically mounted. Any number of additional bearings or seals may be incorporated in a given analysis.

[1] Numbers in brackets designate References at end of paper.

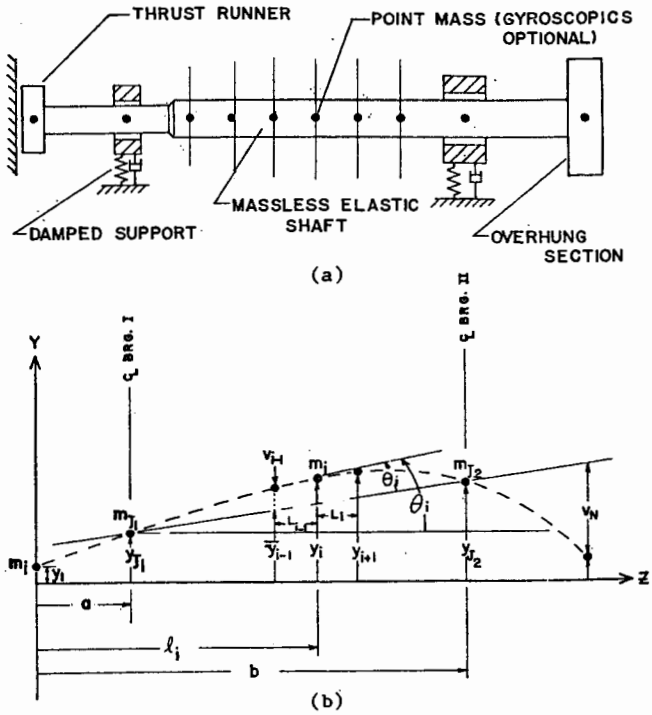

Fig. 1 (a) Multimass rotor simulation for analytic modeling; (b) deflection nomenclature for a multimass flexible rotor

The rotor station deflections will be denoted by the deflections relative to the main bearing center line (u_i, v_i) and also by the corresponding absolute deflections (x_i, y_i). These are shown in Fig. 1(*b*) for the y-coordinate deflection in the y-z plane. The relative and absolute angular displacements for the ith rotor station are also shown in Fig. 1(*b*). Angular displacements of each disk will be denoted by the angles θ_y, which is a rotation in the y-z plane about the negative x-axis and θ_x which is a rotation in the x-z plane about the positive y-axis.

A cross section of the ith mass station is given in Fig. 2 which indicates a possible whirl configuration for the eccentric disk at some instant of time. The absolute and relative deflection nomenclature for the station geometric center, o_g, is illustrated and the displacements of the bearing support and journal are denoted as ($\bar{X}_{si}$, $\bar{Y}_{si}$) and ($\bar{X}_i$, $\bar{Y}_i$), respectively. These deflections, which represent the rigid rotor center line and support center line at this instant in time, are referred from the first bearing location

Nomenclature

l_i = length to ith station along rotor shaft
m_i = mass of ith rotor station $= W_i/g$
m_{J_1}, m_{J_2} = mass of first and second bearing stations
N = rotor speed, rpm
$(P_x, P_y)_i$ = external forces at ith rotor station
Q_i = aerodynamic excitation at ith station
t = time variable
$(u, v)_i$ = relative displacement at ith station
$(x, y)_i$ = absolute displacement at ith station
$(x_J, y_J)_{1,2}$ = bearing station displacement
$(\ddot{X}^{(m)}, \ddot{Y}^{(n)})_i$ = column vector of station accelerations
α_{ij} = flexibility influence coefficient (deflection/load)
β_{ij} = flexibility influence coefficient (deflection/couple)
φ_{ij} = flexibility influence coefficient (rotation/load)
γ_{ij} = flexibility influence coefficient (rotation/couple)
β_{τ_i} = angle between mass station eccentricity vector and maximum skew line in disk
φ = angular relation of mass eccentricity relative to a reference point on shaft
τ = skew of ith rotor station
$(\hat{\theta}_x, \hat{\theta}_y)_i$ = relative angular motion at ith station
$(\theta_x, \theta_y)_i$ = absolute angular motion at ith station
$(\Theta_x^{(n)}, \Theta_y^{(n)})_i$ = column vector of angular rotations
ω = rotor speed

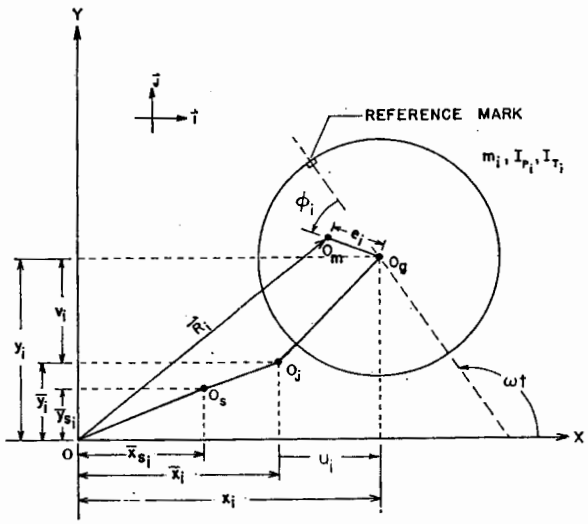

Fig. 2 Cross section of *i*th mass station

as follows:

$$\bar{X}_i = x_{J_1} + \frac{x_{J_2} - x_{J_1}}{b - a} \times [l_i - a] \tag{1}$$

$$\bar{X}_{s_i} = x_{s_1} + \frac{x_{s_2} - x_{s_1}}{b - a} \times [l_i - a] \tag{2}$$

Similar expressions hold for the y-coordinate deflections referred to the ith station.

The relative deflections of the mass stations are assumed to be small so that linearized gyroscopic moments may be used in the equations. The flexibility influence coefficients for the rotor shaft are assumed to remain constant for the order of approximation being considered. Rotor motion in the axial direction is assumed to be negligible and the system is assumed to be torsionally rigid.

Equations of Motion

Rotor Equations. The equations of motion of a flexible rotor may be written in terms of the well-known flexibility influence coefficients which are easily derived from simple beam theory for stepped axisymmetric rotor shafting [6]. The resulting equation may be expressed in the following matrix notation (see Appendix):

$$\begin{bmatrix} \ddot{X}^{(n)} \\ \hline \ddot{\theta}_x{}^{(n)} \end{bmatrix} = \begin{bmatrix} A & B \\ \hline C & D \end{bmatrix}^{-1} \begin{bmatrix} F_x{}^{(n)} \\ \hline \Theta_x{}^{(n)} \end{bmatrix} \tag{3}$$

$$\begin{bmatrix} \ddot{Y}^{(n)} \\ \hline \ddot{\theta}_y{}^{(n)} \end{bmatrix} = \begin{bmatrix} A & B \\ \hline C & D \end{bmatrix}^{-1} \begin{bmatrix} F_y{}^{(n)} \\ \hline \Theta_y{}^{(n)} \end{bmatrix} \tag{4}$$

These equations express the absolute acceleration of the rotor stations in terms of the matrix product of the inverse of the modified flexibility coefficients and a column vector of displacements calculated by taking into account all forces acting on the shafting.

The external forces and moments acting on the shaft may be the result of any combination of the following excitations:

1 Rotor imbalance at each station which results from eccentric or warped shafting.

2 Aerodynamic excitation created by blade-tip clearance variation around the circumference of the rotor span [7].

3 Internal friction damping caused by shrink-fits, bolted sections, and to a lesser degree, in various other rotor shafting [8, 9].

4 Gyroscopic moments created by whirling massive stations that include contributions due to steady synchronous whirl as well as couples caused by rotor acceleration and skewed disks [6, 10].

5 Shaft absolute damping created by windage and interaction with the working fluid of compressors or turbine stations.

6 Forces created by hydrodynamic fluid-film bearings and seals along the rotor shaft.

Bearing Equations. The previous equations are all that are necessary when considering a flexible rotor on two rigid bearing supports. If the bearings or supports are allowed to have flexibility, then additional information must be obtained to solve the resulting dynamic system. The necessary equations are obtained by considering total shaft moments about the bearing supports and are expressed as follows:

$$\ddot{x}_{J_2} = \frac{1}{m_{J_2}} \left\{ (\text{B.F.})_{x_2} + \frac{1}{b - a} \left(\sum_{i=1}^{n} C_{y_i} + \sum_{i=1}^{n} P_{x_i}(l_i - a) \right) \right\} \tag{5}$$

$$\ddot{y}_{J_2} = \frac{1}{m_{J_2}} \left\{ (\text{B.F.})_{y_2} + \frac{1}{b - a} \left(\sum_{i=1}^{n} C_{x_i} + \sum_{i=1}^{n} P_{y_i}(l_i - a) \right) \right\} \tag{6}$$

$$\ddot{x}_{J_1} = \frac{1}{m_{J_1}} \left\{ (\text{B.F.})_{x_1} + \frac{1}{b - a} \left(- \sum_{i=1}^{n} C_{y_i} + \sum_{i=1}^{n} P_{x_i}(b - l_i) \right) \right\} \tag{7}$$

$$\ddot{y}_{J_1} = \frac{1}{m_{J_1}} \left\{ (\text{B.F.})_{y_1} + \frac{1}{b - a} \left(- \sum_{i=1}^{n} C_{x_i} + \sum_{i=1}^{n} P_{y_i}(b - l_i) \right) \right\} \tag{8}$$

Bearing and/or seal forces at stations other than the foregoing two bearing stations enter the solution by equations (3) and (4).

Support Equations. When the bearings are supported by flexibly mounted structures, the equations of the supports are readily deduced by a force balance on the bearing support structure. Isolated support structures are most easily handled but more complex representation which would account for continuous case structure may be formulated using rigid-body equations of motion. If the case structure is flexible then equations similar to equations (3) and (4) would be formulated for the case structure and solved concurrently with the rotating structure member solution.

Method of Solution

The rotor equations of motion as presented in equations (3), and (4) are expressed in terms of absolute acceleration rates and are thus in the proper form for application of standard integration procedures. The solution of the initial value problem may be calculated for consecutive time steps if all displacements and velocities are known at some reference time, t_0. These initial displacements and velocities allow the acceleration rates of all coordinates at the reference time to be calculated which then allows the velocities and displacements at time $t_0 + \Delta t$ to be calculated.

Standard procedure is to either

1 Consider all coordinates at zero condition and introduce external forces to drive the system either to a steady-state solution or in a sustained transient whirl mode of vibration.

2 Calculate the system steady-state conditions (by Prohl-type solution) and start the solution near these calculated conditions.

The latter would be desirable for studies of stability of forced response and the former for studies of blade loss impact or for large perturbation stability studies.

The acceleration rate of the rotor shaft is accounted for in the transient solution by calculating the speed at each time step from specified angular acceleration rates. Thus

$$\omega_t = \omega_{t-\Delta t} + \int_{t-\Delta t}^{t} \dot{\omega} dt \tag{9}$$

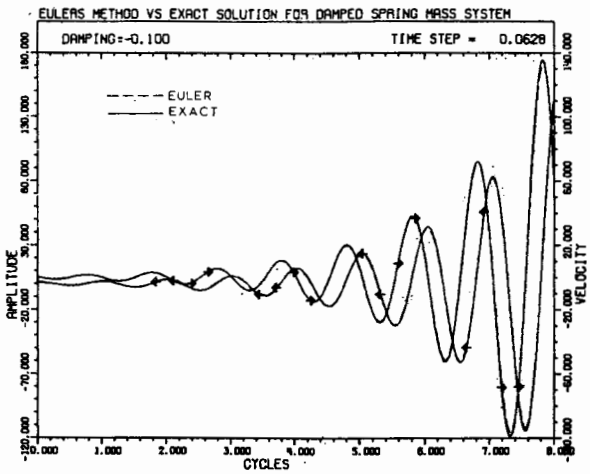

Fig. 3 Euler's integration procedure showing velocity and displacement compared to exact solution for a damped spring-mass system

For a constant acceleration rate, this is simply expressed as

$$\omega_t = \omega_{t-\Delta t} + \dot{\omega}\Delta t \tag{10}$$

The external torques may also be specified to allow the angular acceleration rate to be calculated.

The equations of interest are second-order differential equations of the general form

$$\frac{d^2x_i}{dt^2} = f(X^{(n)}, Y^{(n)}, \dot{X}^{(n)}, \dot{Y}^{(n)}, \theta_x{}^{(n)}, \theta_y{}^{(n)}, \dot{\theta}_x{}^{(m)}, \dot{\theta}_y{}^{(n)}) = \bar{F} \tag{11}$$

The solution of this type equation is then obtained as the solution of two first-order equations; that is,

$$\frac{dV_i}{dt} = \bar{F} \tag{12}$$

$$\frac{dx_i}{dt} = V_i \tag{13}$$

Numerous numerical schemes have been investigated for solution of rotor dynamics time transient simulation. The methods are classed as either (*a*) self-starting procedures or (*b*) predictor-corrector procedures (these require a starting procedure based on type (*a*) to begin the solution).

The most basic self-starting method is simply a Taylor series expansion truncated after two terms which is known as Euler's method. When this concept is applied to the foregoing equation, the result is as follows:

$$V_i(t) = V_i(t - \Delta t) + \Delta t\bar{F} \tag{14}$$

$$x_i(t) = x_i(t - \Delta t) + \Delta t V_i(t) \tag{15}$$

Fig. 3 compares the Euler solution of a simple negative damped spring mass system. Both the Euler and the exact solutions are on the plot and only a very slight deviation from the exact solution is evident after seven cycles of response. Both velocity and displacement are plotted on the same graph for the Euler (dashed line) and the exact solution (solid line).

More elaborate equations can be developed by using finite-difference methods. Other self-starting equations are second-order Runge-Kutta, fourth-order Runge-Kutta, and sixth-order Runge-Kutta. The more elaborate the integration scheme, the more time is required for each time step solution. The time of solution must be at a minimum while retaining accuracy and hence the simpler schemes are very attractive if their accuracy can be assured.

The predictor-corrector equations are applied in an iterative manner until they agree to within desired limits at the given time t, then the approach is repeated for the next time increment. The Milne predictor-corrector pair and the Hammings method have each proven to exhibit high levels of numerical instability when used for the solution of rotor bearing transient response. Some success has been achieved using the Adam's predictor-corrector formulation:

Predictor:

$$V_i(t) = V_i(t - \Delta t) + \frac{\Delta t}{24}(55\bar{F}(t - \Delta t) - 59\bar{F}(t - 2\Delta t) + 37\bar{F}(t - 3\Delta t) - 9\bar{F}(t - 4\Delta t)) \tag{16}$$

Corrector:

$$V_i(t) = V_i(t - \Delta t) + \frac{\Delta t}{24}(9\bar{F}(t) + 19\bar{F}(t - \Delta t) - 5\bar{F}(t - 2\Delta t) + \bar{F}(t - 3\Delta t) \tag{17}$$

The foregoing equations are typical of the predictor-corrector-type formulations. The proper choice of the method of solution

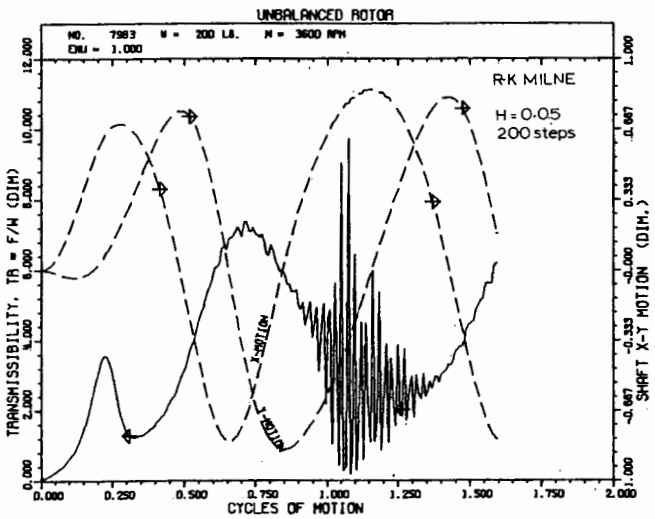

Fig. 4 Dynamic response calculated by Milne predictor-corrector method showing severe numerical instability in force calculation

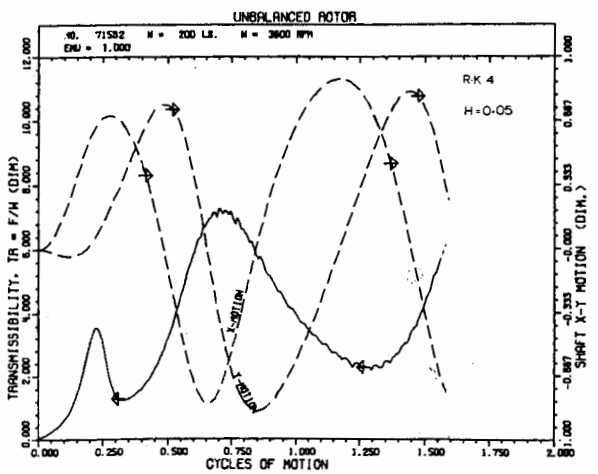

Fig. 5 Dynamic response calculated by 4th-order Runge-Kutta procedure showing small numerical instability in force calculation

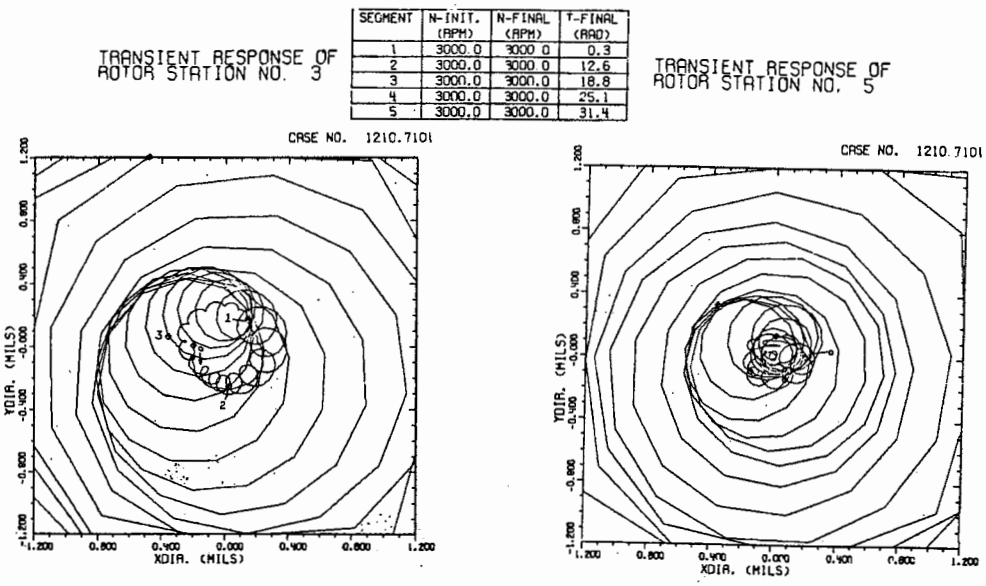

Fig. 6 *Transient response of overhung rotor showing instability developed from higher mode participation*

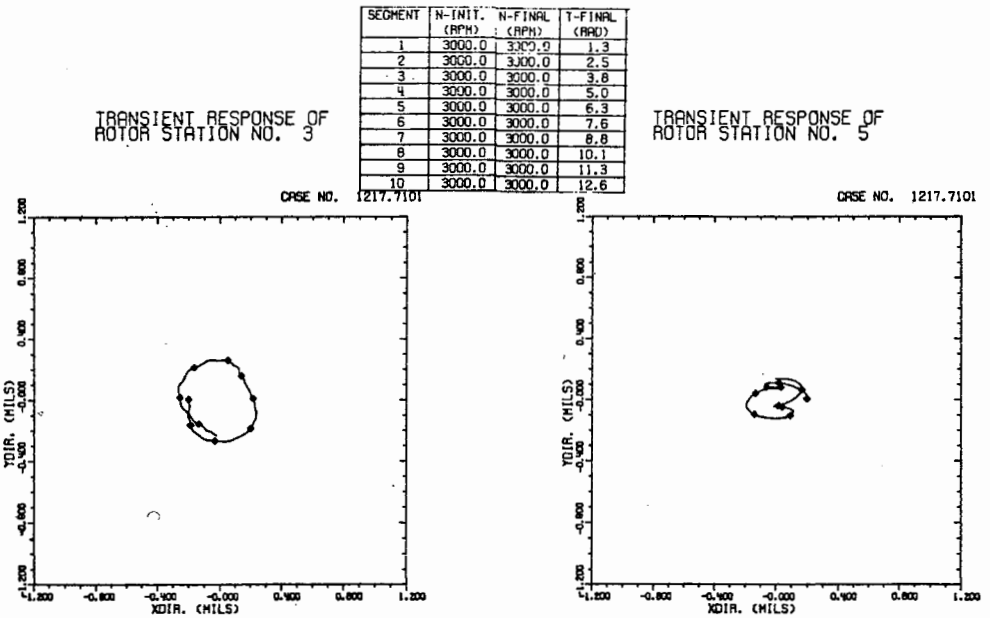

Fig. 7 *Correct transient response of overhung rotor obtained by reducing time step to track high-frequency response*

is very difficult and has proven to be dependent upon the particular problem being solved. As an example, while testing several of the methods on a simple sine wave, the Milne equation gave excellent results. However, upon applying the same method to rotor-bearing equation, violent oscillations occurred indicating numerical instability whereas the Euler equation with comparable time step gave very smooth response prediction. Fig. 4 gives an indication of the numerical instability which may be encountered in a predictor-corrector-type solution and Fig. 5 gives the same response as calculated by a fourth-order Runge-Kutta procedure. Oscillations appear first in the acceleration (force) calculations and are smoothed out by integration so that the displacements are the last quantity to show instability (numerical). Therefore, checks for numerical instability should be made on the acceleration calculations and not the displacement calculations. Other forms of instability may appear in multi-degree-of-freedom systems. For these systems the transient solution allows the response to contain vibratory motion that is composed of contributions from each natural mode. Hence, if shock excitation excites a very high-frequency response and the time step is not sufficiently small to accurately track this motion, then the solution may grow in an unbounded response. Improper starting conditions of either amplitude or phase relationship can excite this type of numerical instability. For example, an overhung turbine location having unnatural initial conditions excited the motion as shown in Fig. 6. The overhung turbine had been

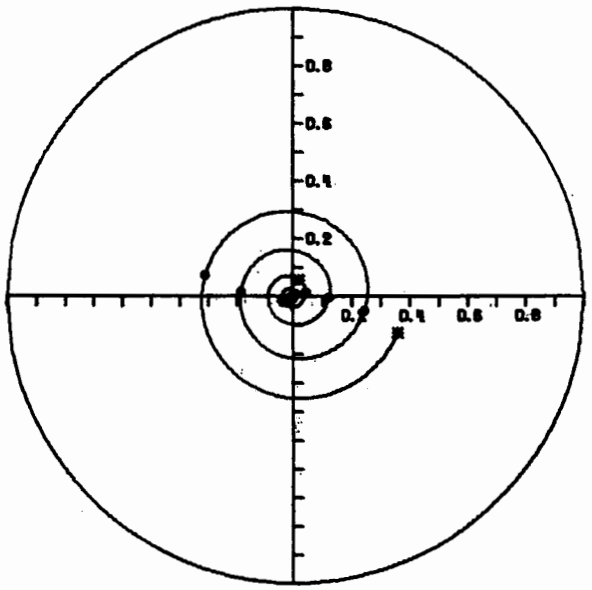

Fig. 8 Journal orbit of a balanced vertical rotor for 10 cycles showing exponential growth of half-frequency whirl

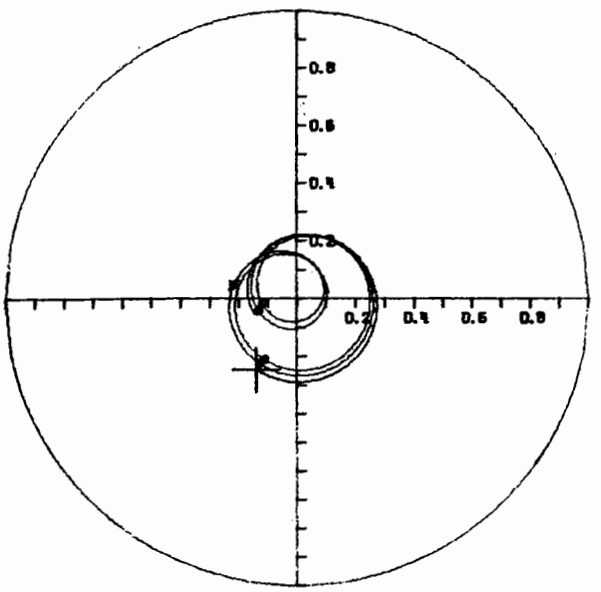

Fig. 9 Journal orbit of vertical rotor with required imbalance to force system to synchronous response

excited at its angular natural frequency which was 10 times running speed and the solution process was given time steps small enough to track only synchronous excitation. The correct solution is indicated in Fig. 7 where two complete cycles of numerically stable solution was calculated using a reduced time step increment.

Extreme caution must be exercised when the system simulation model is being developed. The model should include only the degrees of freedom necessary to give the dynamic response information at the particular running speed range being investigated. High-speed simulation is best suited to transient response and allows many degrees of freedom to be included in the simulation model. Low-speed simulation requires that either (*a*) the degrees of freedom be reduced to avoid numerical difficulties or (*b*) extremely small time steps be used to assure a valid solution.

The results of the many cases run to date indicate that the simple Euler integration scheme is well suited to rotor dynamic transient response calculations. The addition of a time step change option to allow initial impact transient tracking with small time steps and gradual time-step increases as the motion "smooths out" would make the scheme very attractive for systems having nonlinear fluid-film bearings. The fluid-film bearing calculations can be very time-consuming and the more elaborate integration schemes require multiple force calculations for each time step.

The fourth-order Runge-Kutta integration method is also very attractive for rotor simulation and has been used with success for multiple-degree-of-freedom systems.

Regardless of the scheme used for solution generation there is a need to check at all times for possible numerical instabilities which appear in the acceleration calculations. Smooth acceleration rates are generally a good sign of accurate dynamic simulation.

Test cases run to date indicate that a time step small enough to give 100 increments per cycle of possible response frequency is necessary to assure an acceptable solution for shock load conditions. Synchronous response requires only 100 steps per cycle of running speed and would be sufficient for verification of small perturbation stability boundaries.

Examples of Transient Response for Rotor Simulation

The useful purposes of transient simulation were outlined in the Introduction. The following two example cases are given to illustrate the usefulness of transient analysis in rotor bearing design and analysis of system performance.

Example 1. The full journal bearing is known to be stable while operating in the horizontal (loaded) position up to a known stability threshold at which condition the well-known half-frequency whirl is excited [5]. The unloaded (vertical) full journal is known to be completely unstable except for the dead center position. Any slight disturbance will initiate an unstable whirl motion. This condition is shown in Fig. 8 where the journal orbit of an unloaded bearing is spiraling outward in the clearance circle with a half-frequency whirl as indicated by the timing marks on the orbit path which represent consecutive cycles of running speed. The introduction of a given imbalance level gives a response as shown in Fig. 9 where the motion is observed to be composed of both a synchronous and half-synchronous component with the motion tending toward a stable synchronous orbit. This fact could not be predicted from standard stability criteria but is readily studied by transient simulation.

Example 2. Fig. 10 illustrates the motion obtained on an overhung centrifugal compressor which exhibited instability due to aerodynamic forces. The rotor was supported by ball bearings mounted in flexible supports. The figure represents the experimental rotor motion obtained by the use of inductance probes at the compressor and coupling ends. Notice that the rotor passes through two resonant speeds at 17,000 and 35,600 rpm. It is of interest to note that at the lower critical speed, a superharmonic oscillation with small excitation of the second critical speed was obtained. The second critical speed was not excited when increasing in rotor speed, but only when the rotor was decreasing in speed. When the compressor discharge pressure ratio was increased at 52,000 rpm, the rotor went into a self-sustained whirl instability which increased with the loading on the compressor wheel until destruction resulted. Fig. 11 represents the rotor orbits for increasing values of pressure ratio as observed on a scope as the test was in progress.

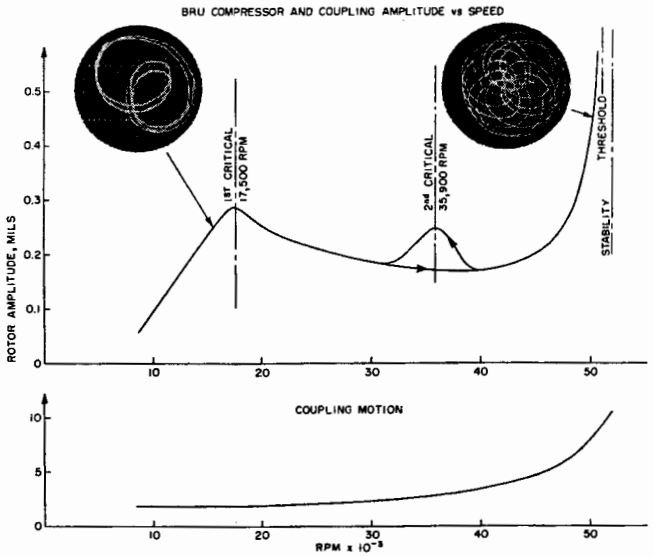

Fig. 10 Amplitude of motion of an overhung centrifugal compressor from 0 to 52,000 rpm

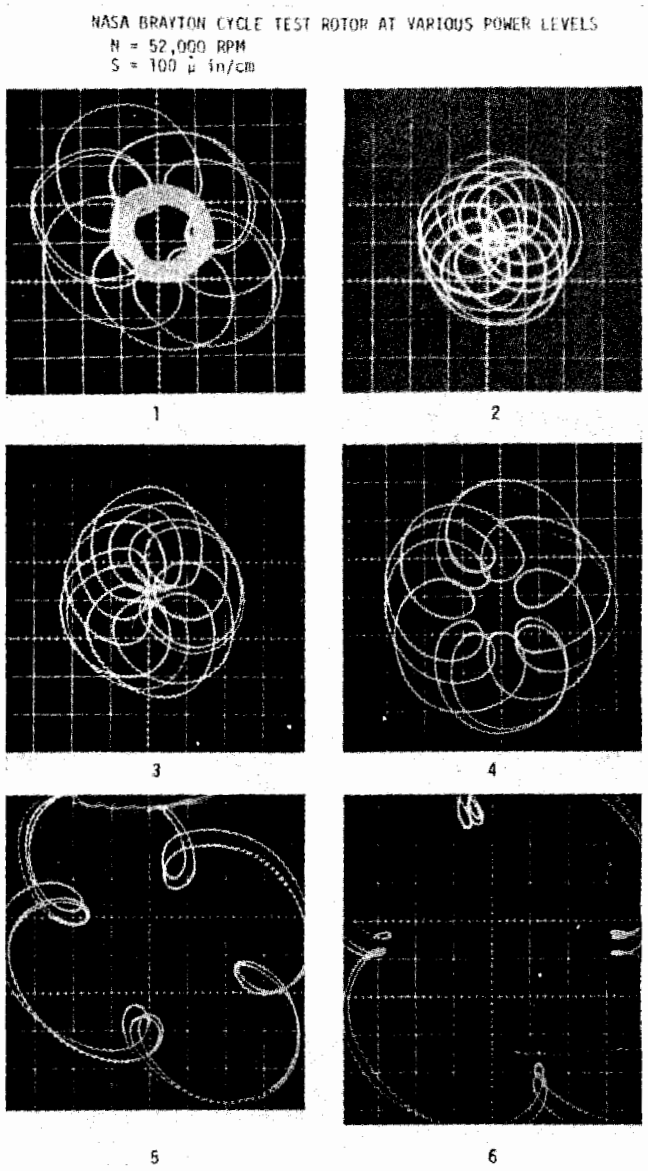

Fig. 11 Compressor motion at 52,000 rpm under increasing discharge pressure ratio

To analyze this motion, critical speed calculations of the flexible rotor were obtained for various values of bearing stiffness. For the flexible support stiffness of 60,000 lb/in, the predicted critical speeds were 17,500 and 35,200 rpm. The rotor synchronous response was evaluated by assuming values of imbalance at the compressor and coupling. The predicted rotor amplitudes at the compressor and coupling due to imbalance was similar to the experimented data below 52,000 rpm. However, the steady-state response calculations could not explain the whirl as observed experimentally. In order to evaluate the nonsynchronous rotor whirl motion observed at 52,000 rpm, the complete transient motion of the flexible rotor was evaluated by computer simulation. Fig. 12 indicates the transient orbit which was obtained when a fixed level of aerodynamic excitation was introduced into the simulation model. The motion is very similar to the experimentally observed orbit pattern and hence it was verified that aerodynamic coupling was the likely cause of the instability in the compressor. At this point in the analysis the transient response computer code could be used to design a damped support system to suppress the instability [6].

Recommendations and Conclusions

The results given in the very simple example rotor systems demonstrate some of the capabilities of the transient flexible rotor response theory. While it would be very desirable to treat a large number of rotor stations (i.e., 50–100), many numerical difficulties arise immediately which prohibit unlimited extension of the number of stations monitored. The analysis incorporates an inverse routine for the modified total flexibility matrix which must be nonsingular and well conditioned. An ill-conditioned flexibility matrix indicates that a lesser number of stations would be valid for system simulation. Hence proper selection of the rotor stations is essential to the solution process. The number of stations allowable is dependent on the relative flexibility of the shaft, the mass and gyroscopic properties, and the speed of operation relative to the system criticals.

The one other point of concern in the solution process is the accuracy of the time integration scheme and the required time step for numerical stability. The numerous cases run to date indicate that a time step capable of accurately tracking the highest natural frequency in the system is essential for impact loading studies. The initial transient solution is composed of a summation of all the modes of the system and hence the solution process must be able to account for all such motion accurately. The inclusion of undamped angular degrees of freedom have caused numerical stability problems which can be avoided by the addition of small amounts of damping for the shaft angular degrees of freedom.

The system solution for a single shaft is readily extended to a multiple shaft rotor-bearing system. Each shaft would be characterized by its own flexibility matrix and the resulting solution would require N such flexibility matrices for an N shaft system. The boundary conditions and shaft interconnecting specifications would enter the solution on the right-hand side of equations similar to equations (3) and (4).

The following major conclusions have been drawn from the application of the theory as presented:

1 Multimass rotor transient simulation may be obtained from the theory as developed in this presentation. Rotors consisting of flexible spans and nonlinear bearing characteristics may be analyzed for stability, steady-state response, and impact loading.

2 Studies of the effect of cross-coupled aerodynamic forces on

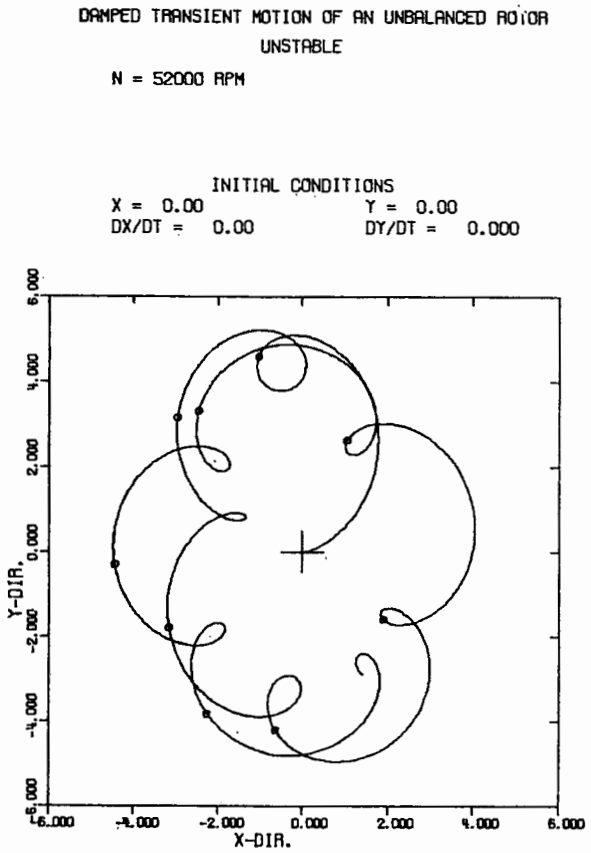

Fig. 12 Transient response of compressor obtained from computer simulation of aerodynamic instability (N = 52,000 rpm)

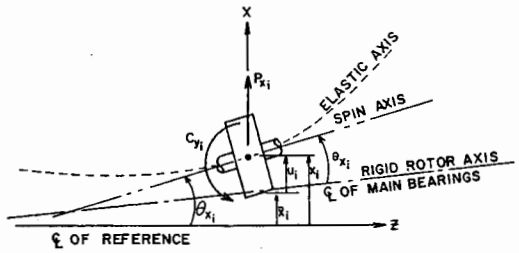

Fig. 13 Force and moment sign convention at ith rotor station

rotor shafts may be simulated by calculating Q terms for selected rotor stations by equations similar to those of Alford [7] or by assuming certain levels of aerodynamic excitation.

3 Blade loss studies for multibearing rotor systems composed of multimass flexible rotors can be studied for maximum force transmission and rotor shaft bending.

4 Proper selection of solution time increment is essential to the numerical stability of the solution and should be small enough to properly track the highest frequency in the system when studying impact loading ($\Delta t \approx 2\pi/(100.0\ \omega_{cr/highest})$).

5 Extension of the analysis to include additional flexible rotor shafting or case structures can be formulated by the present theory. Since the initial conditions on displacement and velocity must be specified to start the solution, no complex boundary condition criteria need be formulated as is necessary for steady-state solution of interconnecting shafting.

6 Extensive experimental testing on scale rotor dynamics rigs must be carried out in conjunction with computer simulation to develop criteria as to the degree of participation of higher and lower modes in the response to impact loading such as that caused by blade loss.

Acknowledgment

The research described herein was conducted at the University of Virginia under NASA Research Grant NGR 47-005-050 with W. J. Anderson, Chief of Bearings Branch, Fluid System Components Division, NASA Lewis Research Center, as technical manager. The authors wish to express their appreciation to Mr. Anderson for his assistance and support in the development of this work.

APPENDIX

A flexible rotor shaft may be represented as a series of stations such as the isolated disk shown in Fig. 13. The equation for external loading due to transverse loads and moments may be derived for each station by application of energy methods. The total kinetic, potential, and dissipative energy for the ith rotor station are expressed as follows [6, 10]:

Kinetic Energy

$$T_i = \Big\{\tfrac{1}{2}m\Big((\dot{x} - e\omega\sin(\omega t + \varphi))^2 + (\dot{y} + e\omega\cos(\omega t + \varphi))^2\Big) + \tfrac{1}{2}I_P\omega(\dot{\theta}_x\theta_y - \dot{\theta}_y\theta_x) + \tfrac{1}{2}I_T(\dot{\theta}_x^2 + \dot{\theta}_y^2) + \frac{\omega^2}{2}(I_P(1-\tau^2) + I_{PT}\tau^2) + \tau\omega(I_T - I_P)(\dot{\theta}_x\cos(\omega t + \varphi + \beta_\tau) + \dot{\theta}_y\sin(\omega t + \varphi + \beta_\tau))\Big\}_i \quad (18)$$

Potential Energy

$$V_i = \{\tfrac{1}{2}K(x^2 + y^2) + \tfrac{1}{2}\mathcal{K}(\theta_x^2 + \theta_y^2)\}_i \quad (19)$$

Dissipative Energy

$$D_i = \{\tfrac{1}{2}c(\dot{x}^2 + \dot{y}^2) + CI(\dot{u}^2 + \dot{v}^2 + 2\omega(v\dot{u} - u\dot{v})) + Q(y\dot{x} - x\dot{y}) + C_\theta(\dot{\theta}_x^2 + \dot{\theta}_y^2)\}_i \quad (20)$$

The equation of motion of the isolated station are easily derived from Lagrange's equation

$$\frac{d}{dt}\left(\frac{\partial T}{\partial \dot{q}}\right) - \frac{\partial T}{\partial q} + \frac{\partial V}{\partial q} + \frac{\partial D}{\partial \dot{q}} = \text{generalized force}|_q \quad (21)$$

These equations applied to the foregoing energy terms would then represent the total force balance on the system with the exception of the flexible shaft influence. The total loading at the ith station in the q-coordinate direction may then be expressed as

$$\text{External loading}|_q = -\frac{d}{dt}\left(\frac{\partial T}{\partial \dot{q}}\right) + \frac{\partial T}{\partial q} - \frac{\partial V}{\partial q} - \frac{\partial D}{\partial \dot{q}} + (\text{Generalized forces}) \quad (22)$$

For example in the x-direction:

$$-\frac{d}{dt}\left(\frac{\partial T_i}{\partial \dot{x}_i}\right) + \frac{\partial T_i}{\partial x_i} - \frac{\partial V_i}{\partial x_i} - \frac{\partial D_i}{\partial \dot{x}_i} + \hat{F}_{x_i} = P_{x_i} \quad (23)$$

where $\hat{F}_x$ = external nonlinear forces developed by shaft reaction with surrounding structures (bearing, seals, etc.).

For the θ_{x_i}-coordinate

$$-\frac{d}{dt}\left(\frac{\partial T_i}{\partial \dot{\theta}_{x_i}}\right) + \frac{\partial T_i}{\partial \theta_{x_i}} - \frac{\partial V_i}{\partial \theta_{x_i}} - \frac{\partial D_i}{\partial \dot{\theta}_{x_i}} = C_{y_i} \quad (24)$$

Similar equations hold for the y_i and $-\theta_{y_i}$-coordinates and are denoted as P_{y_i} and C_{x_i}, respectively.

The equations of motion including the flexible shaft are then written in terms of the flexibility influence coefficients by expressing the relative deflections and angular rotations as follows:

$$u_i = \alpha_{ij}P_{xj} + \beta_{ij}C_{yj} \tag{25}$$

$$v_i = \alpha_{ij}P_{yj} - \beta_{ij}C_{xj} \tag{26}$$

$$\hat{\theta}_{xi} = \varphi_{ij}P_{xj} + \gamma_{ij}C_{yj} \tag{27}$$

$$\hat{\theta}_{yi} = \varphi_{ij}P_{yj} - \gamma_{ij}C_{xj} \tag{28}$$

where

$$P_{xj} = (-m\ddot{x} - c\dot{x} - Kx + me\omega^2 \cos(\omega t + \varphi) + me\dot{\omega} \sin(\omega t + \varphi) - CI\dot{u} - \omega CIv - Qy + \hat{F}_x)_j = -m_j\ddot{x}_j + \mathfrak{F}_{xj} \tag{29}$$

$$P_{yj} = (-m\ddot{y} - c\dot{y} - Ky + me\omega^2 \sin(\omega t + \varphi) - me\dot{\omega} \cos(\omega t + \varphi) - CI\dot{v} + \omega CIu + Qx - W + \hat{F}_y)_j = -m_j\ddot{y}_j + \mathfrak{F}_{yj} \tag{30}$$

$$C_{xj} = (I_T\ddot{\theta}_y - \omega I_P\dot{\theta}_x - \tfrac{1}{2}I_P\dot{\omega}\theta_y - (I_P - I_T)\tau\omega^2 \times \sin(\omega t + \varphi + \beta_\tau) - \tau\dot{\omega}(I_P - I_T)\cos(\omega t + \varphi + \beta_\tau) + C_\theta\dot{\theta}_y + \mathcal{K}\theta_y)_j = I_T\ddot{\theta}_{yj} + H_{xj} \tag{31}$$

$$C_{yj} = (-I_T\ddot{\theta}_x - \omega I_P\dot{\theta}_y - \tfrac{1}{2}I_P\dot{\omega}\theta_x + (I_P - I_T)\tau\omega^2 \cos(\omega t + \varphi + \beta_\tau) - \tau\dot{\omega}(I_P - I_T)\sin(\omega t + \varphi + \beta_\tau) - C_\theta\dot{\theta}_x - \mathcal{K}\theta_x)_j = -I_T\ddot{\theta}_{xj} + H_{yj} \tag{32}$$

By removing the inertia terms from the foregoing equations, the acceleration terms may be expressed as a product of known values for each time step. The equations are expressed as

$$\begin{bmatrix} A & B & 0 & 0 \\ C & D & 0 & 0 \\ 0 & 0 & A & B \\ 0 & 0 & C & D \end{bmatrix} \begin{bmatrix} \ddot{X}^{(n)} \\ \ddot{\theta}_x{}^{(m)} \\ \ddot{Y}^{(m)} \\ \ddot{\theta}_y{}^{(m)} \end{bmatrix} = \begin{bmatrix} F_x{}^{(n)} \\ \Theta_x{}^{(n)} \\ F_y{}^{(n)} \\ \Theta_y{}^{(n)} \end{bmatrix} \tag{33}$$

$$A_{ij} = \alpha_{ij}m_j \tag{34}$$

$$B_{ij} = \beta_{ij}I_{Tj} \tag{35}$$

where

$$C_{ij} = \varphi_{ij}m_j \tag{36}$$

$$D_{ij} = \gamma_{ij}I_{Tj} \tag{37}$$

with

$$\ddot{X}^{(n)} \equiv \begin{bmatrix} \ddot{x}_1 \\ \ddot{x}_2 \\ \cdot \\ \cdot \\ \cdot \\ \ddot{x}_n \end{bmatrix}; \quad \ddot{Y}^{(n)} \equiv \begin{bmatrix} \ddot{y}_1 \\ \ddot{y}_2 \\ \cdot \\ \cdot \\ \cdot \\ \ddot{y}_n \end{bmatrix}; \quad \ddot{\theta}_x{}^{(m)} \equiv \begin{bmatrix} \ddot{\theta}_{x_1} \\ \cdot \\ \cdot \\ \cdot \\ \ddot{\theta}_{x_n} \end{bmatrix}; \quad \ddot{\theta}_y{}^{(m)} \equiv \begin{bmatrix} \ddot{\theta}_{y_1} \\ \cdot \\ \cdot \\ \cdot \\ \ddot{\theta}_{y_n} \end{bmatrix}$$

and (38)

$$F_x{}^{(n)} \equiv \begin{bmatrix} -u_1 + \alpha_{1j}\mathfrak{F}_{xj} + \beta_{1j}H_{yj} \\ \cdot \\ \cdot \\ \cdot \\ -u_n + \alpha_{nj}\mathfrak{F}_{xj} + \beta_{nj}H_{yj} \end{bmatrix} \tag{39}$$

$$\Theta_x{}^{(n)} \equiv \begin{bmatrix} -\hat{\theta}_{x1} + \varphi_{1j}\mathfrak{F}_{xj} + \gamma_{1j}H_{yj} \\ \cdot \\ \cdot \\ \cdot \\ -\hat{\theta}_{xn} + \varphi_{nj}\mathfrak{F}_{xj} + \gamma_{nj}H_{yj} \end{bmatrix} \tag{40}$$

$$F_y{}^{(n)} \equiv \begin{bmatrix} -v_1 + \alpha_{1j}\mathfrak{F}_{yj} - \beta_{1j}H_{xj} \\ \cdot \\ \cdot \\ \cdot \\ -v_n + \alpha_{nj}\mathfrak{F}_{yj} - \beta_{nj}H_{xj} \end{bmatrix} \tag{41}$$

$$\Theta_y{}^{(n)} = \begin{bmatrix} -\hat{\theta}_{y1} + \varphi_{1j}\mathfrak{F}_{yj} - \gamma_{1j}H_{xj} \\ \cdot \\ \cdot \\ \cdot \\ -\hat{\theta}_{yn} + \varphi_{nj}\mathfrak{F}_{yj} - \gamma_{nj}H_{xj} \end{bmatrix} \tag{42}$$

This formulation then gives the complete equations of motion necessary to express the total dynamic response of the torsionally rigid, flexible, multimass rotor.

References

1 Shen, F. A., "Transient Flexible-Rotor Dynamic Analysis—Part 1: Theory," JOURNAL OF ENGINEERING FOR INDUTRY, TRANS. ASME, Vol. 94, Series B, No. 2, May 1972, pp. 531–538.

2 Childs, D. W., "A Simulation Model for Flexible Rotating Equipment," JOURNAL OF ENGINEERING FOR INDUSTRY, TRANS. ASME, Vol. 94, Series B, No. 1, Feb. 1972, pp. 201–209.

3 Badgley, R. H., and Booker, J. F., "Turborotor Instability: Effect of Initial Transient on Plane Motion," *Journal of Lubrication Technology*, TRANS. ASME, Vol. 91, Series F, No. 3, Oct. 1969, pp. 625–633.

4 Akers, A., Michaelson, S., and Cameron, A., "Stability Contours for a Whirling Finite Journal Bearing," *Journal of Lubrication Technology*, TRANS. ASME, Vol. 93, Series F, No. 1, Jan. 1971, pp. 177–190.

5 Kirk, R. G., and Gunter, E. J., "Transient Journal Bearing Analysis," NASA CR-1549, Washington, D. C., June 1970.

6 Kirk, R. G., and Gunter, E. J., "Nonlinear Transient Analysis of Multimass Flexible Rotors," RLES Report ME 4040-110-72 U, University of Virginia, June 1972.

7 Alford, J. S., "Protecting Turbomachinery From Self-Excited Rotor Whirl," *Journal of Engineering for Power*, TRANS. ASME, Series A, Vol. 87, Oct. 1965, pp. 333–344.

8 Gunter, E. J., "The Influence of Internal Friction on the Stability of High-Speed Rotors," JOURNAL OF ENGINEERING FOR INDUSTRY, TRANS. ASME, Vol. 89, Series B, Nov. 1967, pp. 683–688.

9 Kirk, R. G. and Gunter, E. J., "The Effect of Support Flexibility and Damping on the Synchronous Response of a Singlemass Flexible Rotor," JOURNAL OF ENGINEERING FOR INDUSTRY, TRANS. ASME, Vol. 94, Series B, No. 1, Feb. 1972, pp. 221–232.

10 Yamamoto, T., "On the Critical Speeds of a Shaft," *Memoirs of the Faculty of Engineering*, Nogoya University, Japan, Nov. 1954, Vol. 6, No. 2, pp. 106–174.

Printed in U. S. A.